

Experimental and theoretical investigations of CB_8^- : towards rational design of hypercoordinated planar chemical species

Boris B. Averkiev,^a Lei-Ming Wang,^{bc} Wei Huang,^{bc} Lai-Sheng Wang^{*bc} and Alexander I. Boldyrev^{*a}

Received 6th May 2009, Accepted 28th July 2009

First published as an Advance Article on the web 9th September 2009

DOI: 10.1039/b908973j

We demonstrated in our joint photoelectron spectroscopic and *ab initio* study that wheel-type structures with a boron ring are not appropriate for designing planar molecules with a hypercoordinate central carbon based on the example of CB_8 , and CB_8^- clusters. We presented a chemical bonding model, derived from the adaptive natural density partitioning analysis, capable of rationalizing and predicting planar structures either with a boron ring or with a carbon atom occupying the central hypercoordinate position. According to our chemical bonding model, in the wheel-type structures the central atom is involved in delocalized bonding, while peripheral atoms are involved in both delocalized bonding and two-center two-electron (2c–2e) σ -bonding. Since carbon is more electronegative than boron it favors peripheral positions where it can participate in 2c–2e σ -bonding. To design a chemical species with a central hypercoordinate carbon atom, one should consider electropositive ligands, which would have lone pairs instead of 2c–2e peripheral bonds. Using our extensive chemical bonding model that considers both σ - and π -bonding we also discuss why the AlB_9 and FeB_9^- species with octacoordinate Al and Fe are the global minima or low-lying isomers, as well as why carbon atom fits well into the central cavity of CAI_4^{2-} and CAI_5^+ . This represents the first step toward rational design of nano- and subnano-structures with tailored properties.

1. Introduction

Continuous miniaturization in electronic devices requires rational design of nano- and subnano-structures. However, there are no simple chemical rules, such as the Lewis model in organic chemistry, for designing novel nano-structures with tailored properties. One attempt has been made recently to develop a simple structural model for boron and mixed carbon–boron clusters.^{1–4} This model assumes that there is a peripheral ring of boron atoms bonded by classical two-center two-electron (2c–2e) bonds with interior atoms bonded to the peripheral ring through delocalized bonding, which can be understood in terms of σ - and π -aromaticity (double aromaticity), σ - and π -antiaromaticity (double antiaromaticity), σ -aromaticity and π -antiaromaticity, and σ -antiaromaticity and π -aromaticity (conflicting aromaticity). We assess aromaticity in chemical species on the basis of the presence of delocalized bonding in cyclic structures. We have recently developed a new tool adaptive natural density partitioning (AdNDP) method⁵ for assessing delocalized bonding in chemical species. This method leads to partitioning of the charge density into elements with the highest possible degree of localization of electron

pairs. If some part of the density cannot be localized in this manner, it is represented using completely delocalized objects, similar to canonical MOs, naturally incorporating the idea of delocalized bonding, *i.e.*, n -center two-electron (nc –2e) bonds. Thus, AdNDP achieves seamless description of different types of chemical bonds and has been applied recently to representative aromatic organic molecules,⁶ as well as boron and gold clusters.^{5,7} If we encounter a molecule or a cluster in which AdNDP analysis reveals that σ - or π -electrons cannot be localized into lone pairs or 2c–2e bonds, we consider such a species from the aromaticity/antiaromaticity point of view. If delocalization occurs over the whole molecule and corresponding bonds satisfy the $4n + 2$ rule we consider such species to be globally aromatic.

The B_9^- molecular wheel (D_{8h} , $^1\text{A}_{1g}$)⁸ is a good example of probing aromaticity using AdNDP analysis (Fig. 1). The B_9^- cluster has 28 valence electrons that form eight 2c–2e peripheral bonds with occupation numbers (ON) 1.96| e | that are close to the ideal 2.00| e | values and six delocalized bonds between the central boron atom and the B_8 ring. The six delocalized bonds are evenly divided between the σ - and π -systems, giving rise to double aromaticity (the delocalized σ -system has 6 electrons satisfying the $4n + 2$ rule for σ -aromaticity and similarly for the delocalized π -system) and nicely explaining the high-symmetry wheel structure of B_9^- .

There is a temptation to substitute isoelectronically the central boron atom in B_9^- by a carbon atom to make a CB_8 wheel structure with the highest coordination number for the central C atom yet known in a planar arrangement. The search

^a Department of Chemistry and Biochemistry, Utah State University, Logan, UT 84322-0300, USA. E-mail: a.i.boldyrev@usu.edu

^b Department of Physics, Washington State University, 2710 University Drive, Richland, WA 99354, USA

^c Chemical & Materials Sciences Division, Pacific Northwest National Laboratory, MS K8-88, P. O. Box 999, Richland, WA 99352, USA. E-mail: ls.wang@pnl.gov

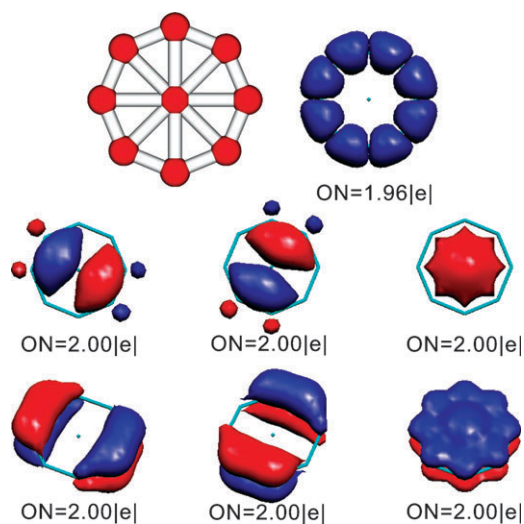


Fig. 1 The global minimum structure of B_9^- (upper left), the eight 2c–2e B–B σ -bonds superimposed over the B_9^- structure (upper right), the three 9c–2e delocalized σ -bonds (middle row), and the three 9c–2e delocalized π -bonds (bottom row), all recovered by the AdNDP analysis.

for high-coordinate planar carbon species started in 1999 and 2000 when we first presented experimental and theoretical evidence of penta-atomic planar coordinated carbon species,^{9–11} which confirmed earlier theoretical predictions.^{12,13} These studies have stimulated renewed interests in designing new tetracoordinate^{14,15} and even hypercoordinate planar carbon molecules.^{16–36} Although none of these species is the global minimum on the potential energy surfaces, it has been suggested that they might be viable experimentally. The three proposed hexa-, hepta-, and octa-coordinated carbon species are the D_{6h} CB_6^{2-} ,¹⁹ D_{7h} CB_7^- ,²⁰ and C_{2v} (effectively D_{8h}) CB_8^{2-} ,²⁴ respectively. The planar CB_6^{2-} cluster with a hexacoordinate carbon has been touted as a “divining molecule” highlighted on the cover of *Chem. Eng. News*.¹⁴ We have shown in previous joint experimental and theoretical investigations that the hypercoordinate D_{6h} CB_6^{2-} (ref. 4) and D_{7h} CB_7^- (ref. 3) clusters are highly unstable and that carbon avoids the central position and therefore hypercoordination in those species as well. Pei and Zeng³⁷ computed the planar tetra-, penta-, hexa-, hepta-, and octa-coordinated structures in carbon–boron mixed clusters and again found that in all the species tested carbon avoids hypercoordination. However, up to now there is no experimental proof that there exists a planar global minimum or planar low-lying isomer of the CB_8 cluster with a hypercoordinated carbon atom.

In the current article, we report a joint experimental and theoretical study of CB_8^- and CB_8 . Photoelectron spectroscopy (PES) is used to probe the electronic structure of the CB_8^- anion and compared with *ab initio* studies for both the anion and the neutral cluster. We show that the experimentally observed species is a C_s CB_8^- cluster, in which the C atom replaces a B atom from the edge rather than at the center of the D_{8h} B_9^- molecular wheel. We present a simple chemical bonding explanation why carbon avoids hypercoordination in the mixed B–C clusters. We further propose a method on how to use pencil and paper chemical bonding models for designing

hypercoordinate planar carbon molecules and planar chemical species with other hypercoordinated atoms.

2. Experimental section

The experiment was performed using a magnetic-bottle PES analyzer equipped with a laser vaporization cluster source, details of which can be found elsewhere.^{38,39} The target used to produce CB_8^- was compressed from a mixed powder of 98% isotopically-enriched ^{10}B with $\sim 3\%$ graphite and about 40% gold (to enhance the compressibility). The cluster anions from the source were analyzed using time-of-flight mass spectrometry. The CB_8^- cluster was mass-selected and decelerated before being photodetached by a 193 nm laser beam from an ArF excimer laser. The photoelectron spectra were calibrated by the known spectrum of Au^- . The energy resolution of the apparatus was $\Delta E/E \approx 2.5\%$, *i.e.*, about 25 meV for 1 eV electrons.

The photoelectron spectrum of CB_8^- (Fig. 2) is rather broad and complicated, suggesting either large geometry changes between the anion and the neutral or a cluster with low symmetry. Numerous spectral features are resolved and are labeled in Fig. 2. The experimental vertical detachment energies (VDEs) of the resolved PES bands are given in Table 1 and compared with theoretical values to be discussed below. The calculated VDEs (at TD-B3LYP level) of the first few detachment channels for the lowest energy structure V (Fig. 4) are plotted as vertical bars in Fig. 2 for comparison.

3. Theoretical calculations of CB_8 and CB_8^- and comparison with experiment

We initially performed searches for the global minimum structure of CB_8 and CB_8^- using a gradient-embedded genetic algorithm (GEGA) program^{40,41} with the B3LYP/3-21G method for energy, gradient, and force calculations. We then reoptimized geometries and calculated frequencies for the lowest four (CB_8) and eight (CB_8^-) structures at the B3LYP/6-311+G* level of theory.^{42–44} We also performed single point energy calculations of the four structures of CB_8 and eight structures of CB_8^- at the CCSD(T)/6-311+G(2df) level of

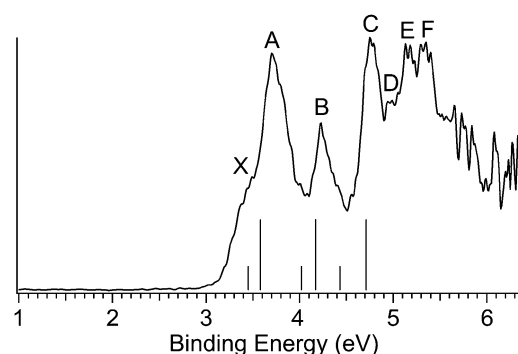


Fig. 2 Photoelectron spectrum of CB_8^- at 193 nm. The vertical bars represent the calculated VDEs (at TD-B3LYP level) for the lowest anion structure. The short bars represent the detachment transitions to singlet neutral states while the longer ones represent transitions to triplet final states.

Table 1 Comparison of the experimental vertical detachment energies (VDE) of CB_8^- with the calculated values for the global minimum C_s structure. All energies are in eV

Feature	VDE (exp.) ^a	Final state and electronic configuration	VDE (theo.)		
			TD-B3LYP ^b	OVGF ^c	$\Delta\text{CCSD(T)}$ ^d
X ^e	~3.45	$^1\text{A}'$, $9a'^2 10a'^2 11a'^2 2a''^2 3a''^2 12a'^0$	3.45	3.69 (0.89)	3.41
A	3.70 (5)	$^3\text{A}''$, $9a'^2 10a'^2 11a'^2 2a''^2 3a''^2 12a'^1$	3.58	3.57 (0.89)	3.72
A tail	~4.0	$^1\text{A}''$, $9a'^2 10a'^2 11a'^2 2a''^2 3a''^1 12a'^1$	4.02	f	f
B	4.23 (4)	$^3\text{A}''$, $9a'^2 10a'^2 11a'^2 2a''^1 3a''^2 12a'^1$	4.17	4.27 (0.88)	f
B tail	~4.5	$^1\text{A}''$, $9a'^2 10a'^2 11a'^2 2a''^1 3a''^2 12a'^1$	4.43	f	f
C	4.75 (5)	$^3\text{A}'$, $9a'^2 10a'^2 11a'^1 2a''^2 3a''^2 12a'^1$	4.71	4.93 (0.88)	4.80
D	~5	$^3\text{A}'$, $9a'^2 10a'^1 11a'^2 2a''^2 3a''^2 12a'^1$	5.06	5.17 (0.87)	f
E	5.16 (5)	$^1\text{A}'$, $9a'^2 10a'^2 11a'^1 2a''^2 3a''^2 12a'^1$	5.48	f	f
F	5.35 (5)	$^3\text{A}'$, $9a'^1 10a'^2 11a'^2 2a''^2 3a''^2 12a'^1$	5.66	5.80 (0.86)	f

^a Numbers in the parentheses represent uncertainties in the last digit. ^b The first two VDEs were calculated at the B3LYP/6-311+G(2df)//B3LYP/6-311+G* level of theory as the lowest transition from the doublet state of the anion into the final lowest singlet and triplet states of the neutral species. Then the vertical excitation energies of the neutral species in the lowest singlet and triplet states (at the TD-B3LYP level) were added to the first two VDEs, respectively, in order to obtain higher VDEs. ^c UOVGF/6-311+G(2df)//B3LYP/6-311+G*. Pole strength is given in parentheses. ^d UCCSD(T)/6-311+G(2df)//B3LYP/6-311+G*. ^e The adiabatic detachment energy (ADE) was estimated to be 3.2 ± 0.1 eV. ^f This VDE cannot be calculated at this level of theory.

theory^{45–47} using the B3LYP/6-311+G* optimized geometries and then corrected the obtained energy values for zero-point energy at B3LYP/6-311+G* (CCSD(T)/6-311+G(2df)//B3LYP/6-311+G*+ZPE//B3LYP/6-311+G*). We found that isomer I (Fig. 3) is the global minimum, in agreement with the result by Pei and Zeng.³⁷ The closest isomer II was found to be $20.4 \text{ kcal mol}^{-1}$ (here and thereafter the relative energies in the text refer to CCSD(T)/6-311+G(2df)//B3LYP/6-311+G*+ZPE//B3LYP/6-311+G*). We found that the high-symmetry structure IV with the putative octacoordinate carbon is a second-order saddle point consistent with previous calculations by Minkin *et al.*²⁴ Optimization following the imaginary frequencies led to isomer III, which is significantly higher ($71.2 \text{ kcal mol}^{-1}$) than the global minimum. The GEGA search for the doublet CB_8^- anion revealed that isomer V (Fig. 4) is the global minimum, in agreement with the results reported by Pei and Zeng.³⁷ There are two low-lying isomers VI and VII, whereas other isomers (VIII–XI) are found to be significantly higher in energy. Again, the high-symmetry structure XII with an octacoordinate carbon is unstable with five imaginary frequencies and it was found to be $116.8 \text{ kcal mol}^{-1}$ higher than the global minimum structure.

The CB_8^- VDEs for the lowest three isomers were calculated using the R(U)CCSD(T)/6-311+G(2df) method, the outer-valence green function method^{48–51} (UOVGF/6-311+G(2df)),

and the time-dependent DFT method^{52,53} (TD B3LYP/6-311+G(2df)) at the B3LYP/6-311+G* geometries. VDEs for isomer V are found to be in excellent agreement with the experimental ones (Table 1). The large geometry changes between the lowest CB_8^- structure V and the neutral CB_8 structure I are consistent with the broad spectrum observed (Fig. 2). As shown in Table 1, all the calculated VDEs are in good agreement with the experimental data. The CCSD(T) values for the X, A, and C channels are in quantitative agreement with the experimental values. VDEs for isomers VI and VII (see Tables 2 and 3) do not agree well with the experimental data.

However, due to the broad nature of the experimental spectrum, we could not completely rule out the presence of isomers VI and VII. But their contributions to the observed spectrum, if any, were expected to be small.

All calculations were performed *via* the Gaussian03 program.⁵⁴ Molecular structures were visualized using MOLDEN3.4 program⁵⁵ and the AdNDP bonds visualization was performed using MOLEKEL, Version 4.3.⁵⁶

4. Chemical bonding analysis

To understand why the structures with an octacoordinate C for CB_8 and CB_8^- are unstable we performed the AdNDP

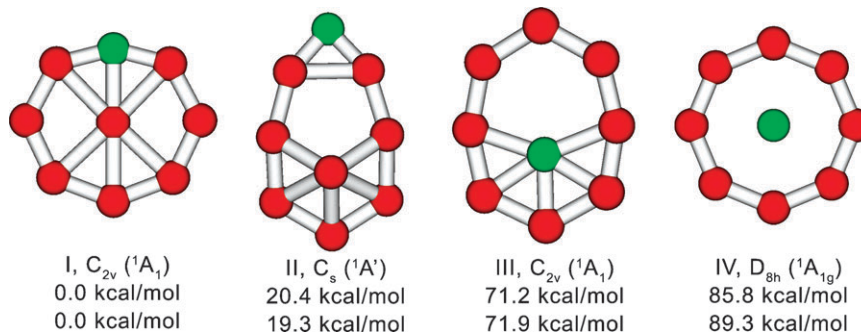


Fig. 3 Selected optimized structures of CB_8 . Upper and lower numbers are relative energies calculated at the CCSD(T)/6-311+G(2df)//B3LYP/6-311+G*+ZPE//B3LYP/6-311+G* and B3LYP/6-311+G*+ZPE//B3LYP/6-311+G* levels of theory, respectively.

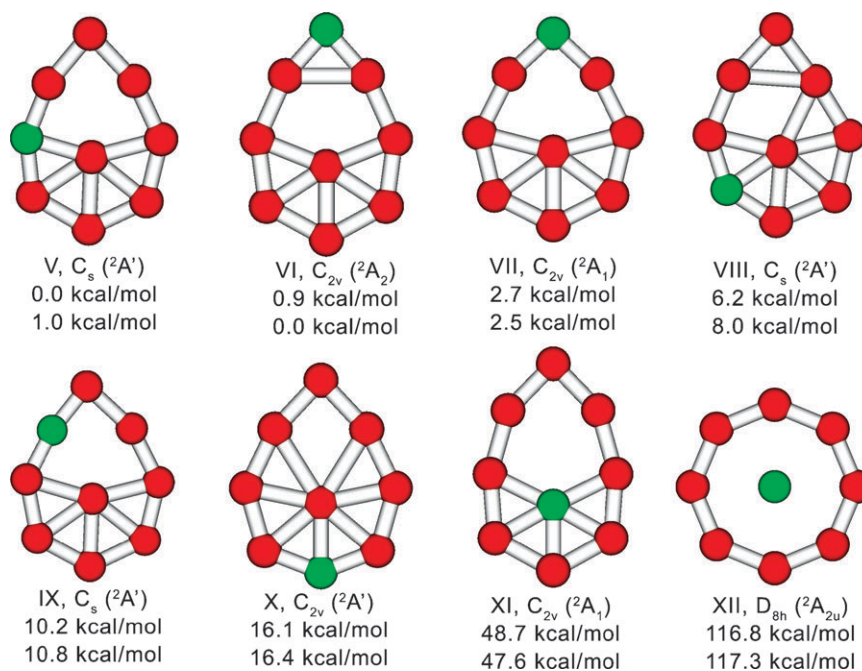


Fig. 4 Selected optimized structures of CB_8^- . Upper and lower numbers are relative energies calculated at the CCSD(T)/6-311+G(2df)//B3LYP/6-311+G*+ZPE//B3LYP/6-311+G* and B3LYP/6-311+G*+ZPE//B3LYP/6-311+G* levels of theory, respectively.

Table 2 Calculated vertical detachment energies (VDE) of CB_8^- for structure VI

Final state and electronic configuration	VDE (calc)/eV		
	TD-B3LYP ^a	OVGf ^b	Δ CCSD(T) ^c
$^3A_2, 6a_1^2 5b_2^2 2b_1^2 7a_1^1 1a_2^1$	3.56	3.56 (0.88)	3.66
$^1A_2, 6a_1^2 5b_2^2 2b_1^2 7a_1^1 1a_2^1$	3.69	<i>d</i>	<i>d</i>
$^1A_1, 6a_1^2 5b_2^2 2b_1^2 7a_1^0 1a_2^0$	3.80	3.91 (0.89)	3.81
$^3B_1, 6a_1^2 5b_2^2 2b_1^2 7a_1^2 1a_2^1$	4.79	5.07 (0.87)	4.86
$^3B_2, 6a_1^2 5b_2^2 2b_1^1 7a_1^2 1a_2^1$	4.91	5.17 (0.87)	5.09
$^1B_2, 6a_1^2 5b_2^2 2b_1^1 7a_1^2 1a_2^1$	5.15	<i>d</i>	<i>d</i>
$^1B_1, 6a_1^2 5b_2^2 2b_1^2 7a_1^2 1a_2^1$	5.20	<i>d</i>	<i>d</i>
$^1A_2, 6a_1^1 5b_2^2 2b_1^2 7a_1^1 1a_2^1$	5.51	<i>d</i>	<i>d</i>
$^3A_2, 6a_1^1 5b_2^2 2b_1^2 7a_1^1 1a_2^1$	5.34	5.69 (0.84)	<i>d</i>

^a The first two VDEs were calculated at the B3LYP/6-311+G(2df)//B3LYP/6-311+G* level of theory as the lowest transition from the doublet state of the anion into the final lowest singlet and triplet states of the neutral species. Then the vertical excitation energies of the neutral species in the lowest singlet and triplet states (at the TD-B3LYP level) were added to the first two VDEs, respectively, in order to obtain higher VDEs. ^b UOVGF/6-311+G(2df)//B3LYP/6-311+G*. Pole strength is given in parentheses. ^c UCCSD(T)/6-311+G(2df)//B3LYP/6-311+G*. ^d This VDE cannot be calculated at this level of theory.

Table 3 Calculated vertical detachment energies (VDE) of CB_8^- for structure VII

Final state and electronic configuration	VDE (calc)/eV		
	TD-B3LYP ^a	OVGf ^b	Δ CCSD(T) ^c
$^3A_2, 1b_1^2 6a_1^2 5b_2^2 2b_1^2 7a_1^1 1a_2^1$	3.20	3.23	3.36
$^1A_2, 1b_1^2 6a_1^2 5b_2^2 2b_1^2 7a_1^1 1a_2^1$	3.46	<i>d</i>	<i>d</i>
$^1A_1, 1b_1^2 6a_1^2 5b_2^2 2b_1^2 7a_1^0 1a_2^2$	3.93	3.99	3.76
$^3B_2, 1b_1^2 6a_1^2 5b_2^2 2b_1^2 7a_1^1 1a_2^2$	4.66	4.61	4.79
$^3B_1, 1b_1^2 6a_1^2 5b_2^2 2b_1^1 7a_1^1 1a_2^2$	4.76	4.81	4.87
$^1B_1, 1b_1^2 6a_1^2 5b_2^2 2b_1^1 7a_1^1 1a_2^2$	5.10	<i>d</i>	<i>d</i>
$^3A_1, 1b_1^2 6a_1^1 5b_2^2 2b_1^2 7a_1^1 1a_2^2$	5.13	5.18	<i>d</i>
$^1B_2, 1b_1^2 6a_1^1 5b_2^2 2b_1^2 7a_1^1 1a_2^2$	5.18	<i>d</i>	<i>d</i>

^a The first two VDEs were calculated at the B3LYP/6-311+G(2df)//B3LYP/6-311+G* level of theory as the lowest transition from the doublet state of the anion into the final lowest singlet and triplet states of the neutral species. Then the vertical excitation energies of the neutral species in the lowest singlet and triplet states (at the TD-B3LYP level) were added to the first two VDEs, respectively, in order to obtain higher VDEs. ^b UOVGF/6-311+G(2df)//B3LYP/6-311+G*. Pole strength is given in parentheses. ^c UCCSD(T)/6-311+G(2df)//B3LYP/6-311+G*. ^d This VDE cannot be calculated at this level of theory.

analysis of chemical bonding in these species at the HF/3-21G level of theory. It was shown previously that the results of the AdNDP analysis similar to that of the natural bonding orbital analysis do not depend on the choice of the basis set.⁶

According to our AdNDP analysis, the chemical bonding in the D_{8h} CB_8 structure IV is identical to that of B_9^- (Fig. 1): they both are doubly (σ - and π -) aromatic systems (6 delocalized σ -electrons and 6 delocalized π -electrons) with eight peripheral 2c–2e B–B bonds (Fig. 5a). However, unlike B_9^- , the D_{8h} CB_8 is not even a minimum because the carbon atom is too small to make a perfect fit into the B_8 ring. Therefore, it is important to take into account the geometric factors in designing highly coordinated planar molecules. The bonding pattern in isomer III (Fig. 5c) that is obtained by following the imaginary frequency mode of the structure IV is somewhat different from the bonding pattern of the high-symmetry structure IV (Fig. 5a). Although the eight peripheral 2c–2e B–B bonds (Fig. 5a–1 and 5c–1) are very similar in both structures, their delocalized σ - and π -bonds are different. The π -bonds in structure IV (Fig. 5a–5–7) are delocalized over the whole cluster, while in isomer III they become one 3c–2e (Fig. 5c–5) and two 4c–2e π -bonds (Fig. 5c–6 and 7). Despite these changes, the partially localized π bonds in isomer III are simply linear combinations of the completely delocalized π -bonds in structure IV. This was confirmed by calculating a slightly distorted structure IV* (Fig. 5b), in which the central carbon atom was shifted by 0.004 Å from the central position. Neither the total energy nor the orbital energies of IV* change significantly from those of IV, but the shape of the π -bonds (Fig. 5b–5–7) in this distorted structure now looks exactly like that in isomer III (Fig. 5c–5–7). Hence, isomer III can be still viewed as a π -aromatic system. However, isomer III is no longer a σ -aromatic system, even though it has three partially delocalized σ -bonds. We found that the σ -bonding pattern of the slightly distorted structure IV* (Fig. 5b–2–4) is different from that of isomer III (Fig. 5c–2–4). The slightly distorted structure IV* is still σ -aromatic, even though the σ -bonds are now partially localized, analogous to the π -bonds discussed above. However, upon further distortion towards isomer III one of the “aromatic” σ -bonds (Fig. 5b–2) is transformed into a new σ -bond (Fig. 5c–2). The three σ -bonds in III (Fig. 5c–2–4) are now localized on the bottom part of the cluster, with the three upper peripheral atoms not participating in the delocalized σ -bonding. Therefore, isomer III is no longer σ -aromatic, while clusters IV and IV* are with all the atoms being involved in delocalized bonding.

This conclusion is confirmed by calculation of NICS_{zz} indices for structures IV and III. In structure IV we found that NICS values are highly negative just above the central carbon atom and they slowly decrease with the height of the probe charge. In structure III, NICS values are highly positive just above the carbon atom, but they become negative with increasing the height of the probe charge. However, III and IV are not low-lying structures. Structure I is the global minimum structure for CB_8 . The reason why isomer I is significantly more stable than structure III and IV can be understood from the bonding patterns. The central C atom in structures III and IV is involved in delocalized bonding with the peripheral atoms only, while in isomer I the C atom is also involved in

2c–2e peripheral bonding with two neighboring boron atoms, in addition to the delocalized bonding. The lower electronegativity of B compared to C clearly favors structures with the peripheral position for the carbon atom. The bonding pattern (Fig. 5d) is almost identical to the bonding pattern of the slightly distorted structure IV* (Fig. 5b) and thus, isomer I is also doubly (σ - and π -) aromatic.

We further performed the AdNDP analysis for the doubly charged CB_8^{2-} anion at the geometry of the global minimum structure V of CB_8^- by adding an electron to the singly occupied HOMO (Fig. 6a). The AdNDP analysis revealed that there are six 2c–2e B–B and two C–B peripheral σ -bonds (Fig. 6a–1), three 3c–2e σ -bonds (Fig. 6a–2–4), one 4c–2e σ -bond (Fig. 6a–5), and two 4c–2e and one 3c–2e π -bonds (Fig. 6a–6–8). The three 3c–2e σ -bonds in structure V of CB_8^{2-} are similar to the three 4c–2e σ -bonds in the slightly distorted octagonal structure of CB_8 (Fig. 5b–2–4). The π -bonds in structure V of CB_8^{2-} are similar to those in the slightly distorted octagonal structure of CB_8 (Fig. 5b–5–7). Finally, 4c–2e σ -bond (Fig. 6a–5) is similar to the 4c–2e σ -bond in the structure III of CB_8 (Fig. 5c–2). As we have already mentioned above, the slightly distorted octagonal structure is still doubly aromatic. The appearance of the extra σ -bond (Fig. 6a–5) makes structure V of CB_8^{2-} σ -antiaromatic with eight σ -electrons participating in the delocalized bonding. We confirmed this conclusion by calculation of NICS over the central boron atom and found that NICS values at low height (0.2 Å and 0.4 Å) are positive and at higher position (0.6 Å, 0.8 Å, 1.0 Å, and 1.2 Å) become negative. These results imply a system with conflicting aromaticity, *i.e.*, σ -antiaromatic and π -aromatic.

5. Rational design of hypercoordinate planar species with an external boron ring

Our previous studies on pure boron clusters^{1,57–59} revealed that in planar structures there is always a peripheral ring of 2c–2e B–B σ -bonds with additional delocalized bonding between peripheral atoms or peripheral atoms and atoms located inside the ring. The presence of this peripheral ring gives us an opportunity to design planar molecules with hypercoordinate central atoms. In order to obtain planar boron clusters with a hypercoordinate central atom, the wheel-type structure has to be a minimum (geometric fit, *i.e.*, structural factor) and the system has also to be doubly aromatic (electronic factor). As we mentioned above, the B_9^- cluster has a D_{8h} wheel structure and it is σ - and π -aromatic. Apparently, the central boron atom fits well into the octagonal B_8 ring. It was shown that ten atomic boron cluster favors the structure in which two boron atoms occupy central positions⁵⁷ and the wheel structure with one central atom located inside the nine-member ring is significantly higher in energy.^{1,2} B_9^- is a system with the highest yet experimentally observed coordination number of 8.

In the CB_6^- , $C_2B_5^-$, CB_6^{2-} , CB_7^- , and CB_8^- clusters, we found that the carbon atom avoids the central position in wheel-type structures. Chemical bonding analysis performed by the AdNDP method revealed that the atom in the central

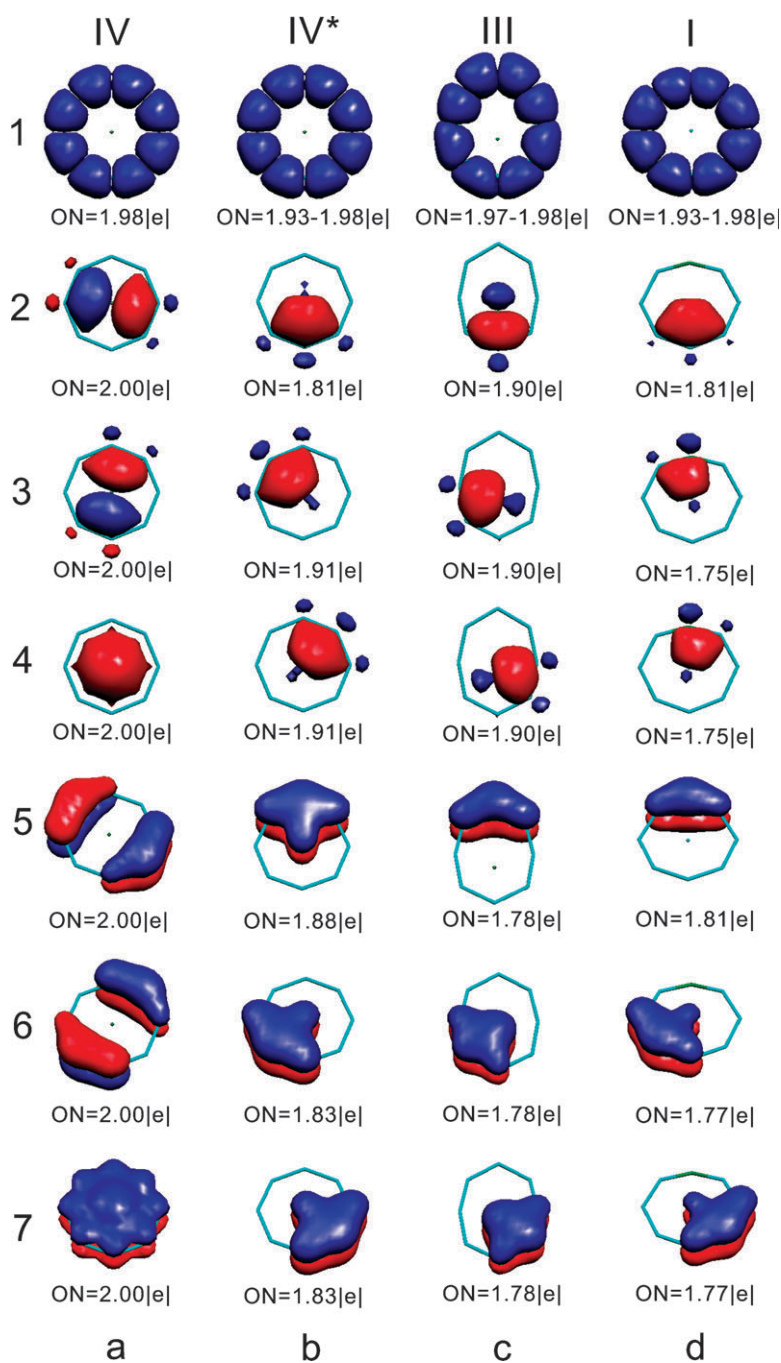


Fig. 5 The eight 2c–2e B–B σ -bonds superimposed over the CB_8 structures (first row), the three delocalized σ -bonds (second to fourth rows), and the three delocalized π -bonds (fifth to seventh rows), recovered by the AdNDP analysis (see text for details).

position in the wheel-type structures is involved in delocalized bonding only, while atoms at the periphery are involved in both delocalized bonding and 2c–2e peripheral σ -bonding. The carbon atom, being more electronegative than the boron atom, favors peripheral positions, where it can participate in 2c–2e σ -bonding. Thus, the boron ring wheel-type structures are not suitable for designing planar molecules with a hypercoordinate central carbon atom.

This observation suggests that atoms, which are more electropositive than boron, may be more viable candidates to sit in a boron ring for hypercoordinate structures. Indeed,

we recently demonstrated⁶⁰ that an aluminium atom can be placed into a B_9 ring to result in a high-symmetry and stable D_{9h} structure, which according to high-level theoretical calculations was shown to be either the global minimum or a low-lying isomer on the potential energy surface. We can readily apply our chemical bonding model described above to the AlB_9 cluster: it possesses 30 valence electrons with 18 electrons participating in nine 2c–2e peripheral B–B σ -bonds, 6 electrons participating in delocalized σ -bonding and 6 electrons participating in delocalized π -bonding (Fig. 7). Thus, AlB_9 is doubly (σ - and π -) aromatic system and Al atom

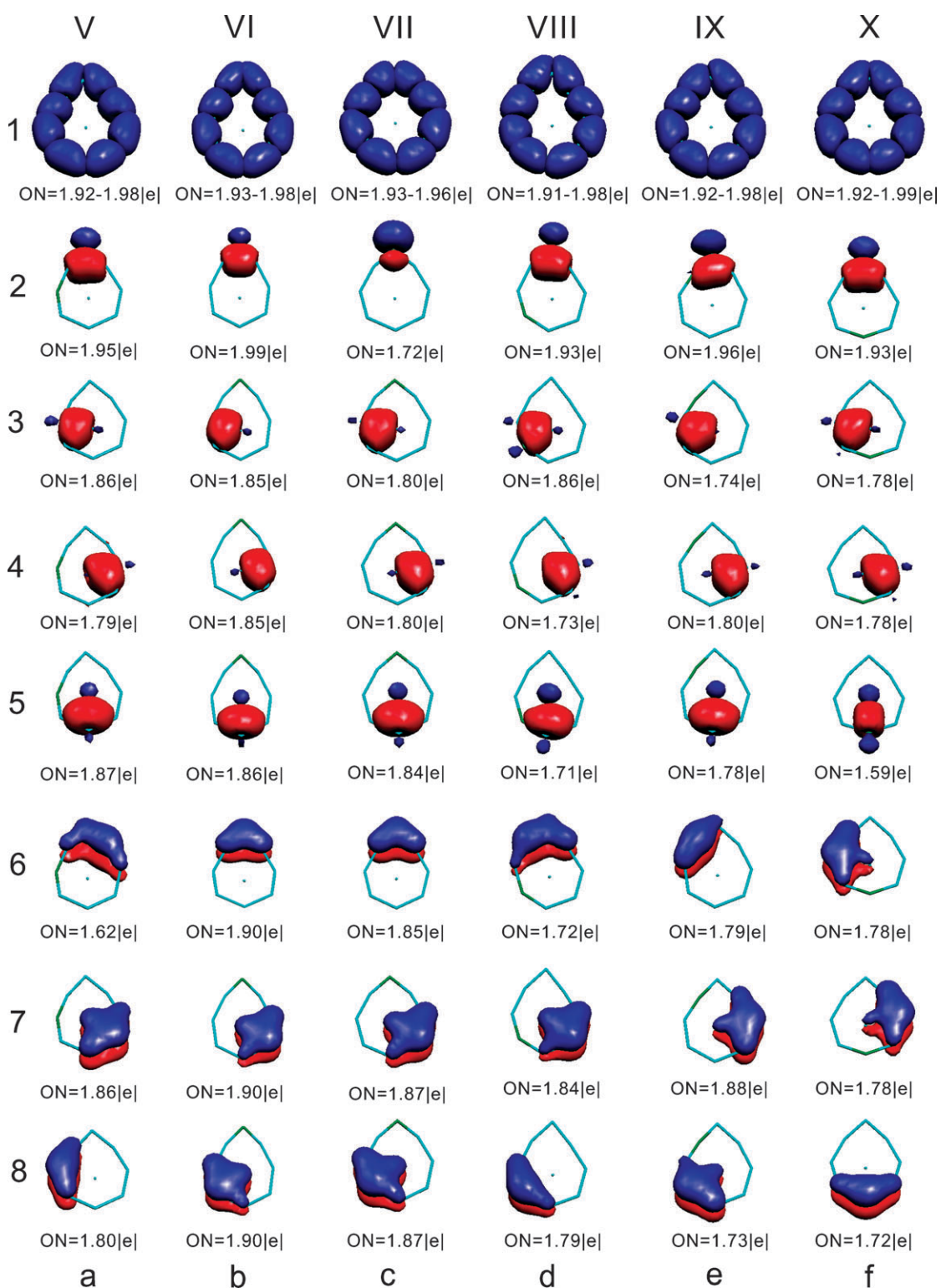


Fig. 6 The eight 2c-2e B-B σ -bonds superimposed over the CB_8^{2-} structures (first row), the four delocalized σ -bonds (second to fifth rows), and the three delocalized π -bonds (sixth to eighth rows), recovered by the AdNDP analysis (see text for details).

is a good geometric fit for the B_9 ring. AlB_9 is the first computationally found system with a nine-coordinate central atom. We tried to use this approach to design a ten-coordinate atom in the AlB_{10}^+ cluster. However, we found that the isomer with Al at the central position of the

B_{10} ring is significantly higher in energy than an alternative isomer, in which the Al^+ cation is located above the B_{10} cluster. We believe that the central cavity for B_{10} is too big to fit favorably the Al^+ cation at the center. Nevertheless, suitable atoms may exist to make ten-coordinate planar clusters.

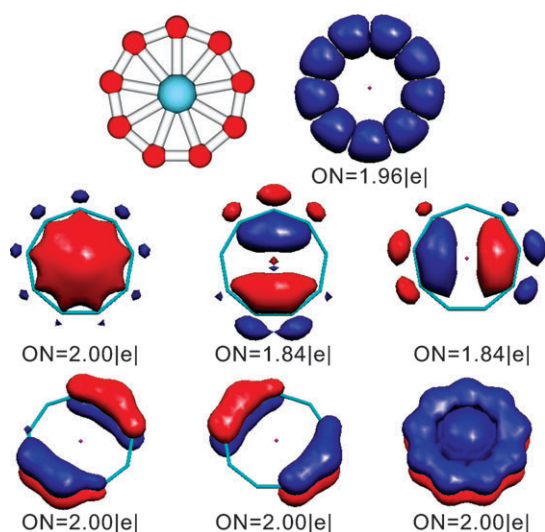


Fig. 7 One of the lowest energy structures of AlB_9 (upper left), its nine 2c–2e B–B σ -bonds superimposed over the AlB_9 structure (upper right), the three 10c–2e delocalized σ -bonds (middle row), and the three 10c–2e delocalized π -bonds (bottom row), all recovered by the AdNDP analysis.

Recently, Ito *et al.*⁶¹ reported a calculation of the global minimum wheel-type FeB_9^- structure with a nine-coordinate Fe atom. This structure can be easily rationalized using our chemical bonding model. The FeB_9^- cluster has 36 valence electrons with 18 electrons participating in nine 2c–2e peripheral B–B σ -bonds, 6 electrons participating in delocalized σ -bonding and 6 electrons participating in delocalized π -bonding, and three pairs of localized 3d electrons on Fe (Fig. 8). Thus, the FeB_9^- cluster is doubly (σ - and π -) aromatic and similar to AlB_9 , the central atom is an electropositive element in agreement with our conclusion that only electropositive (relative to boron) atoms can have high-symmetry global minimum structures or at least to be a low-lying isomer.

6. Rational design of hypercoordinate planar carbon species

In spite of the unfavorable location of a carbon atom in boron rings, it has been shown theoretically and experimentally that carbon occupies the central position in the square of four aluminium atoms in the CAL_4^- (ref. 9) and NaCAL_4^- (ref. 11) species. At first glance, these findings may seem to contradict the previously discussed chemical bonding model. However, our AdNDP analysis performed for the CAL_4^{2-} dianion (Fig. 9) showed that bonding between the peripheral boron atoms in planar wheel structures and those of aluminium atoms in CAL_4^{2-} is quite different. One can see that there are no 2c–2e peripheral Al–Al σ -bonds in CAL_4^{2-} . Instead, there is a lone pair at every aluminium atom (Fig. 9a). There are also two delocalized bonds: one is a 4c–2e peripheral σ -bond composed out of 3p tangential aluminium AOs (Fig. 9f) and another one is a 5c–2e π -bond composed of mainly $2p_z$ -AO of carbon with small contributions from the

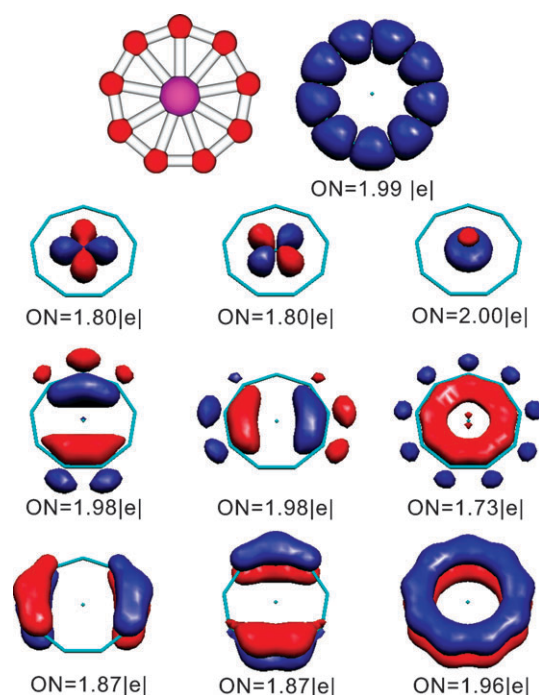


Fig. 8 The global minimum structure of FeB_9 (upper left), its nine 2c–2e B–B σ -bonds superimposed over the FeB_9 structure (upper right), the three pairs of localized 3d electrons (second row), the 9c–2e delocalized σ -bonds (third row), and the three 9c–2e delocalized π -bonds (fourth row), all recovered by the AdNDP analysis.

$3p_z$ -AOs of Al atoms (Fig. 9e). The other three bonds are essentially 2s-AO on C (Fig. 9d) and $2p_x$ - and $2p_y$ -AOs on C (Fig. 9b and c). Thus, bonding in CAL_4^{2-} can be approximately considered as being due to ionic bonding between a central carbon C^{4-} anion and an Al_4^{2+} cation (with significant covalent contribution) and due to the delocalized σ -bonding and weakly delocalized π -bonding. Therefore, in order to design a chemical species with a central hypercoordinate carbon atom, one should consider electropositive ligands, which tend to form lone pairs instead of 2c–2e peripheral bonds. Aluminium is a good example of such a ligand, but it is conceivable that there may exist a class of such atoms to design hypercoordinate carbon species. A recent theoretical prediction of a planar pentacoordinate carbon in the CAL_5^+ cation⁶² provides another example for our design principle.

As considered in our article hypercoordinate chemical species CB_8 , CB_8^- , CAL_5^+ , AlB_9 and FeB_9^- belong to electron deficient hypervalent chemical species.^{63,64} This conclusion can be supported by results of the natural bond analysis (at B3LYP/6-311+G*) that revealed that the charges at the central atoms are the following: $Q(\text{C}) = -0.45|e|$ with the atomic occupations $2s^{1.28}2p^{3.15}$ in CB_8 , $Q(\text{C}) = -2.65|e|$ with the atomic occupations $2s^{1.65}2p^{4.97}$ in CAL_5^+ , $Q(\text{Al}) = 1.46|e|$ with the atomic occupations $3s^{0.44}3p^{1.05}$ in AlB_9 , and $Q(\text{Fe}) = 0.02|e|$ with atomic occupations $4s^{0.21}3d^{7.65}$ in FeB_9^- . The hypervalency in these hypercoordinate species is due to delocalized bonding revealed by our AdNDP analysis and not due to the formation of extra 2c–2e radial bonds.

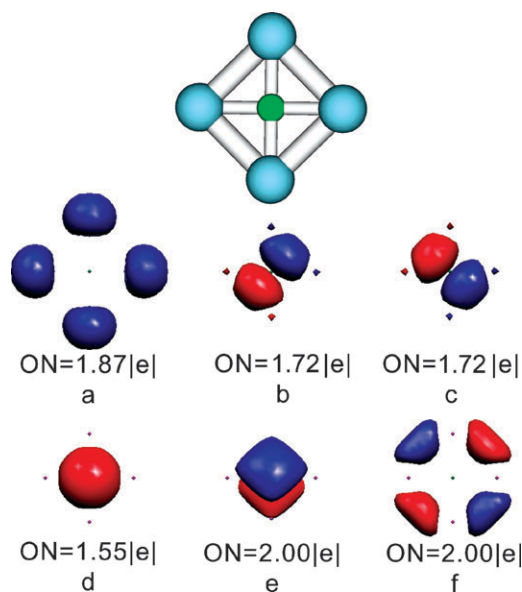


Fig. 9 The structure of CA_{14}^{2-} (top), (a) the four Al lone pairs superimposed over the CA_{14}^{2-} structure, (b and c) the $2p_x$ - and $2p_y$ -AOs of the carbon atom, (d) the $2s$ -AO of the carbon atom, (e) $5c-2e$ delocalized π -bond, and (f) $4c-2e$ σ -tangential bond (all recovered by AdNDP analysis).

7. Summary

From our joint photoelectron spectroscopic and *ab initio* study we have demonstrated that carbon avoids central positions in CB_6^{2-} , CB_7^- , CB_8 , and CB_8^- . We have developed a chemical bonding model (using AdNDP analysis), which explains why carbon avoids the central position in those species. According to this model, in the wheel-type structures the central atom is involved in delocalized bonding only, while atoms at the periphery of the wheel structure are involved in both delocalized bonding and $2c-2e$ peripheral σ -bonding. The carbon atom is more electronegative than boron atoms and favors peripheral positions where it can participate in $2c-2e$ σ -bonding. Thus, wheel-type structures with a boron ring are not appropriate for designing planar molecules with a hypercoordinate central carbon. However, if the central atom is more electropositive than boron, then the wheel-type structures are stable and can be either global minimum or low-lying isomers. The results of the AdNDP analysis of the chemical bonding in the CA_{14}^{2-} dianion showed that in this case, the favorable central position of the carbon atom is due to essentially ionic bonding between a central carbon C^{4-} anion and an Al_4^{2+} cation with contributions from delocalized σ -bonding and weakly delocalized π -bonding. In order to design a chemical species with a central hypercoordinate carbon atom, one should consider electropositive ligands, which would have lone pairs instead of forming $2c-2e$ peripheral bonds. The same is true for the pentacoordinate carbon atom inside the Al_5^+ ring (CA_{15}^+ cluster). We used our extensive chemical bonding model, which considers both σ - and π -electrons to explain why the AlB_9 and FeB_9^- species with octacoordinate Al and Fe are the global minima or low-lying isomers. Though the global minimum structure of FeB_9^- was established by Ito *et al.*,⁶¹ they considered in their chemical bonding analysis only

π -electron. We have shown that σ -electrons are also important for rationalizing high-symmetry and high coordination number of Fe in FeB_9^- . Hence, we presented a comprehensive chemical bonding model capable of rationalizing and predicting structures either with a boron ring or a central planar carbon. This represents the first step towards rational design of nano- and subnano-structures with tailored properties.

Acknowledgements

The theoretical work done at Utah State University was supported by the National Science Foundation (CHE-0714851). Computer time from the Center for High Performance Computing at Utah State University is gratefully acknowledged. The computational resource, the Uinta cluster supercomputer, was provided through the National Science Foundation under Grant CTS-0321170 with matching funds provided by Utah State University. The experimental work done at Washington State University was supported by the National Science Foundation (DMR-0503383) and partly by the donors of the Petroleum Research Fund (ACS PRF# 46275-AC6) administered by the American Chemical Society and was performed at the W. R. Wiley Environmental Molecular Sciences Laboratory, a national scientific user facility sponsored by DOE's Office of Biological and Environmental Research and located at Pacific Northwest National Laboratory, which is operated for DOE by Battelle.

References

- 1 A. N. Alexandrova, A. I. Boldyrev, H.-J. Zhai and L. S. Wang, *Coord. Chem. Rev.*, 2006, **250**, 2811.
- 2 D. Yu. Zubarev and A. I. Boldyrev, *J. Comput. Chem.*, 2007, **28**, 251.
- 3 L.-M. Wang, W. Huang, B. B. Averkiev, A. I. Boldyrev and L. S. Wang, *Angew. Chem., Int. Ed.*, 2007, **46**, 4550.
- 4 B. B. Averkiev, D. Yu. Zubarev, L.-M. Wang, W. Huang, L. S. Wang and A. I. Boldyrev, *J. Am. Chem. Soc.*, 2008, **130**, 9248.
- 5 D. Yu. Zubarev and A. I. Boldyrev, *Phys. Chem. Chem. Phys.*, 2008, **10**, 5207.
- 6 D. Yu. Zubarev and A. I. Boldyrev, *J. Org. Chem.*, 2008, **73**, 9251.
- 7 D. Yu. Zubarev and A. I. Boldyrev, *J. Phys. Chem. A*, 2009, **113**, 866.
- 8 H.-J. Zhai, A. N. Alexandrova, A. I. Boldyrev and L. S. Wang, *Angew. Chem., Int. Ed.*, 2003, **42**, 6004. See also a recent study on the low-lying isomers of B_9^- : L. L. Pan, J. Li and L. S. Wang, *J. Chem. Phys.*, 2008, **129**, 024302.
- 9 X. Li, W. Chen, L. S. Wang, A. I. Boldyrev and J. Simons, *J. Am. Chem. Soc.*, 1999, **121**, 6033.
- 10 L. S. Wang, A. I. Boldyrev, X. Li and J. Simons, *J. Am. Chem. Soc.*, 2000, **122**, 7681.
- 11 X. Li, H.-F. Zhang, L. S. Wang, G. D. Geske and A. I. Boldyrev, *Angew. Chem., Int. Ed.*, 2000, **39**, 3630.
- 12 P. v. R. Schleyer and A. I. Boldyrev, *J. Chem. Soc., Chem. Commun.*, 1991, 1536.
- 13 A. I. Boldyrev and J. Simons, *J. Am. Chem. Soc.*, 1998, **120**, 7967.
- 14 J. Kemsley, *Chem. Eng. News*, 2007, **85**, 17.
- 15 R. Keese, *Chem. Rev.*, 2006, **106**, 4787, and references therein.
- 16 G. Merino, M. A. Mendez-Rojas, A. Vela and T. Heine, *J. Comput. Chem.*, 2007, **28**, 362, and references therein.
- 17 B. Sateesh, A. S. Reddy and G. N. Sastry, *J. Comput. Chem.*, 2007, **28**, 335, and references therein.
- 18 W. Siebert and A. Gunale, *Chem. Soc. Rev.*, 1999, **28**, 367, and references therein.
- 19 K. Exner and P. v. R. Schleyer, *Science*, 2000, **290**, 1937.
- 20 Z.-X. Wang and P. v. R. Schleyer, *Science*, 2001, **292**, 2465.

- 21 S. Erhardt, G. Frenking, Z. Chen and P. v. R. Schleyer, *Angew. Chem., Int. Ed.*, 2005, **44**, 1078.
- 22 K. Ito, Z. Chen, C. Corminboeuf, C. S. Wannere, X. H. Zhang, Q. S. Li and P. v. R. Schleyer, *J. Am. Chem. Soc.*, 2007, **129**, 1510.
- 23 R. Islas, T. Heine, K. Ito, P. v. R. Schleyer and G. Merino, *J. Am. Chem. Soc.*, 2007, **129**, 14767.
- 24 R. M. Minyaev, T. N. Gribanova, A. G. Starikov and V. I. Minkin, *Mendeleev Commun.*, 2001, **11**, 213.
- 25 T. N. Gribanova, R. M. Minyaev and V. I. Minkin, *Russ. J. Inorg. Chem. (Transl. of Zh. Neorg. Khim.)*, 2001, **46**, 1207.
- 26 R. M. Minyaev, T. N. Gribanova, A. G. Starikov and V. I. Minkin, *Dokl. Chem.*, 2002, **382**, 41.
- 27 V. I. Minkin and R. M. Minyaev, *Mendeleev Commun.*, 2004, **14**, 43.
- 28 S.-D. Li, C.-Q. Miao and G.-M. Ren, *Eur. J. Inorg. Chem.*, 2004, 2232.
- 29 S.-D. Li, J.-G. Guo, C.-Q. Miao and G.-M. Ren, *J. Phys. Chem. A*, 2005, **109**, 4133.
- 30 S.-D. Li and C.-Q. Miao, *J. Phys. Chem. A*, 2005, **109**, 7594.
- 31 S.-D. Li, C.-Q. Miao, G.-M. Ren and J.-C. Guo, *Eur. J. Inorg. Chem.*, 2006, 2567.
- 32 S. Shahbazian and A. Sadjadi, *THEOCHEM*, 2007, **822**, 116.
- 33 L.-M. Yang, H.-P. He, Y.-H. Ding and C.-C. Sun, *Organometallics*, 2008, **27**, 1727.
- 34 S. Shahbazian and A. Sadjadi, *J. Phys. Chem. A*, 2008, **112**, 10365.
- 35 Q. Luo, X. H. Zhang, K. L. Huang, S. Q. Liu, Z. H. Yu and Q. S. Li, *J. Phys. Chem. A*, 2007, **111**, 2930.
- 36 S.-D. Li, C.-Q. Miao and J.-C. Guo, *J. Phys. Chem. A*, 2007, **111**, 12069.
- 37 Y. Pei and X. C. Zeng, *J. Am. Chem. Soc.*, 2008, **130**, 2580.
- 38 L. S. Wang, H. S. Cheng and J. Fan, *J. Chem. Phys.*, 1995, **102**, 9480.
- 39 L. S. Wang and X. Li, in *Clusters and Nanostructure Interfaces*, ed. P. Jena, S. N. Khanna and B. K. Rao, World Scientific, River Edge, New Jersey, 2000, pp. 293–300.
- 40 A. N. Alexandrova, A. I. Boldyrev, Y.-J. Fu, X. Yang, X.-B. Wang and L. S. Wang, *J. Chem. Phys.*, 2004, **121**, 5709.
- 41 A. N. Alexandrova and A. I. Boldyrev, *J. Chem. Theory Comput.*, 2005, **1**, 566.
- 42 A. D. Becke, *J. Chem. Phys.*, 1993, **98**, 5648.
- 43 S. H. Vosko, L. Wilk and M. Nusair, *Can. J. Phys.*, 2008, **58**, 1200.
- 44 C. Lee, W. Yang and R. G. Parr, *Phys. Rev. B*, 1988, **37**, 785.
- 45 J. Cizek, *Adv. Chem. Phys.*, 1969, **14**, 35.
- 46 P. J. Knowles, C. Hampel and H.-J. Werner, *J. Chem. Phys.*, 1993, **99**, 5219.
- 47 K. Raghavachari, G. W. Trucks, J. A. Pople and M. Head-Gordon, *Chem. Phys. Lett.*, 1989, **157**, 479.
- 48 L. S. Cederbaum, *J. Phys. B: At. Mol. Phys.*, 1975, **8**, 290.
- 49 J. V. Ortiz, *Int. J. Quantum Chem., Quantum Chem. Symp.*, 1989, **23**, 321.
- 50 J. S. Lin and J. V. Ortiz, *Chem. Phys. Lett.*, 1990, **171**, 197.
- 51 V. G. Zakrzewski, J. V. Ortiz, J. A. Nichols, D. Heryadi, D. L. Yeager and J. T. Golab, *Int. J. Quantum Chem.*, 1996, **60**, 29.
- 52 R. Bauernshmitt and R. Alrichs, *Chem. Phys. Lett.*, 1996, **256**, 454.
- 53 M. E. Casida, C. Jamorski, K. C. Casida and D. R. Salahub, *J. Chem. Phys.*, 1998, **108**, 4439.
- 54 M. J. Frisch, G. W. Trucks, H. B. Schlegel, G. E. Scuseria, M. A. Robb, J. R. Cheeseman, J. A. Montgomery, Jr., T. Vreven, K. N. Kudin, J. C. Burant, J. M. Millam, S. S. Iyengar, J. Tomasi, V. Barone, B. Mennucci, M. Cossi, G. Scalmani, N. Rega, G. A. Petersson, H. Nakatsuji, M. Hada, M. Ehara, K. Toyota, R. Fukuda, J. Hasegawa, M. Ishida, T. Nakajima, Y. Honda, O. Kitao, H. Nakai, M. Klene, X. Li, J. E. Knox, H. P. Hratchian, J. B. Cross, V. Bakken, C. Adamo, J. Jaramillo, R. Gomperts, R. E. Stratmann, O. Yazyev, A. J. Austin, R. Cammi, C. Pomelli, J. Ochterski, P. Y. Ayala, K. Morokuma, G. A. Voth, P. Salvador, J. J. Dannenberg, V. G. Zakrzewski, S. Dapprich, A. D. Daniels, M. C. Strain, O. Farkas, D. K. Malick, A. D. Rabuck, K. Raghavachari, J. B. Foresman, J. V. Ortiz, Q. Cui, A. G. Baboul, S. Clifford, J. Cioslowski, B. B. Stefanov, G. Liu, A. Liashenko, P. Piskorz, I. Komaromi, R. L. Martin, D. J. Fox, T. Keith, M. A. Al-Laham, C. Y. Peng, A. Nanayakkara, M. Challacombe, P. M. W. Gill, B. G. Johnson, W. Chen, M. W. Wong, C. Gonzalez and J. A. Pople, *GAUSSIAN 03 (Revision D.01)*, Gaussian, Inc., Wallingford, CT, 2004.
- 55 G. Schaftenaar, *MOLDEN 3.4*, CAOS/CAMM Center, The Netherlands, 1998.
- 56 S. Portmann, *MOLEKEL Version 4.3*, CSCS/ETHZ, Switzerland, 2002.
- 57 H. J. Zhai, B. Kiran, J. Li and L. S. Wang, *Nat. Mater.*, 2003, **2**, 827.
- 58 B. Kiran, S. Bulusu, H. J. Zhai, S. Yoo, X. C. Zeng and L. S. Wang, *Proc. Natl. Acad. Sci. U. S. A.*, 2005, **102**, 961.
- 59 A. P. Sergeeva, D. Yu. Zubarev, H. J. Zhai, A. I. Boldyrev and L. S. Wang, *J. Am. Chem. Soc.*, 2008, **130**, 7244.
- 60 B. B. Averkiev and A. I. Boldyrev, *Russ. J. Gen. Chem.*, 2008, **78**, 769.
- 61 K. Ito, Z. Pu, Q.-S. Li and P. v. R. Schleyer, *Inorg. Chem.*, 2008, **47**, 10906.
- 62 Y. Pei, W. An, K. Ito, P. v. R. Schleyer and X. C. Zeng, *J. Am. Chem. Soc.*, 2008, **130**, 10394.
- 63 K.-y. Akiba, *Chemistry of Hypervalent Compounds*, Wiley-VCH, New York, 1999.
- 64 I. Fernandes, E. Uggerud and G. Frenking, *Chem.–Eur. J.*, 2007, **13**, 8620.